

Laser-initiated Reactions Of Energetic/Thermitic Composites

Jared C. Gump and Suhithi M. Peiris

Indian Head Division, Naval Surface Warfare Center
101 Strauss Avenue
Indian Head, MD 20640 USA

Abstract: *Researchers are attempting to prepare smaller (nano-scale) metal particles, and nano-scale thermitic (metal–metal-oxide) composites. When added to energetic compositions, these nano-materials could burn during or close behind the shock front produced by an explosive material. Therefore, investigation of their combustion kinetics is important, especially when the investigation technique requires only very small quantities of material that is initially prepared. This study uses time-resolved emission spectroscopy to measure reaction kinetics and mechanisms of micrograms of material initiated by a laser pulse. Results from nano-scale aluminum and the thermite-type compositions of Al+Fe₂O₃, Al+MoO₃, and Al+B₂O₃ are presented here.*

Keywords: *laser, nano-scale, composite, kinetics, time-resolved spectroscopy*

Introduction

Metals such as aluminum have been added to energetic material compositions for a long time. Traditionally the Al particles have been in the 20–100 micrometre range, resulting in Al burning after (or behind) the shock front produced by the energetic material. More recently, researchers have been attempting to prepare smaller (nano-scale) metal particles, and nano-scale thermitic (metal–metal-oxide) composites. These nano-materials could burn during or close behind the shock front produced by an explosive material.^{1–4} It is important to develop a simple method to measure reaction kinetics using the initially prepared small quantities of these new materials. We use time-resolved emission spectroscopy to measure reaction kinetics of microgram quantities of sample. In this paper we present time-resolved reaction data from nano-scale aluminum and the nano-aluminum containing thermite-type compositions of Al+Fe₂O₃, Al+MoO₃, and Al+B₂O₃, and discuss the kinetic rates of these reactive materials.

Experimental Method

Sample holders were prepared by exposing 5 μm gold foil to focused 532 nm laser light from a 5 ns pulsed ND:YAG laser. The resulting holes were on the order of 80–120 μm in diameter. Powdered samples were pressed onto the gold foil hole using

a pestle. Average sample thickness was estimated at 15 μm.

Mounted samples were returned to the focus position of the 532 nm laser and exposed to a single 5 ns pulse. Emitted light was collected and sent by a fiber optic cable first into a spectrometer to disperse the light spatially, then into a streak camera to temporally separate the spectra, and finally into a CCD to measure the intensity of the light at each time and wavelength. The spectrometer was centered at 490 nm and has a spatial range of ~100 nm. The streak camera was set for a 47 μs window. The zero for the time axis was determined by the image of the laser pulse on the streak camera output. Laser pulse energy was estimated from a portion of the beam that was diverted into an energy meter using a single glass slide. For these experiments the average energy per pulse was ~220 mJ.

Experimental results

Nano Al

The energetic/thermitic composites in this study all use nanometre size Al as their fuel. Therefore, it is important to understand what response should be expected from the laser initiation of nano Al by itself. 120.5 nm Al was obtained from Technanogy. This Al had a 4.9 nm thick oxide coating (74.3% active Al content).

During all the laser initiation experiments we performed, an intense, broad background appears in the first couple of microseconds due to the laser interaction with surrounding air. This background reduces after the first couple of microseconds. In the case of nano Al initiation, evidence for AlO emission can be seen above the background noise as early as the first microsecond. By the third microsecond the background has reduced and the dominant features in the spectrum are due to AlO emission. These results are illustrated in Figure 1. Note that due to edge effects on the detector, peaks below about 465 nm in this wavelength window are significantly less intense relative to the rest of the spectrum. The AlO signal that appears by 3 μ s persists until 37 μ s. Beyond that time, any peak intensity has reduced to the level of the background noise. In Figure 1 each line plot was obtained by averaging over spectra within the time range shown in the legend. The stick plot refers to emission lines obtained from spectrographic references.^{5,6} The region from approximately 520–540 nm is reduced in intensity due to a 532 nm notch filter placed in the beam path to reduce the intensity of the exciting laser, which defines time $t = 0$.

Al + Fe₂O₃

A representative set of spectra for an Al + Fe₂O₃

sample prepared by Professor Edward Dreizin (New Jersey Institute of Technology) is shown in Figure 2.⁷ The first peaks attributed to the Al + Fe₂O₃ sample appear above the background even during the first or second microsecond. A full set of peaks is clearly visible beginning from 4 μ s, and the average of the spectra from 4 to 8 μ s is shown. The majority of peaks appearing in this spectrum can be attributed to elemental iron. These results illustrate that the iron oxide is breaking apart very early in the reaction. Some iron lines persist through 30 μ s, but any evidence of them beyond 38 μ s is lost in the background noise.

By 30 μ s there is some evidence for the appearance of AlO peaks. The maximum intensity for these peaks occurs during 30 to 34 μ s. A time average over this interval is shown in Figure 2. As can be seen, the AlO peaks are not well-formed. This may be due in part to overlap with the iron lines that are still in the spectrum.

An Al + Fe₂O₃ sample was also obtained from Professor Michael Zachariah's group (University of Maryland).⁸ This sample also exhibited Fe peaks within the first couple of microseconds after exposure. However, by the 9 μ s peaks from AlO emissions become visible and are more intense than the Fe peaks. The strongest Fe peaks persist

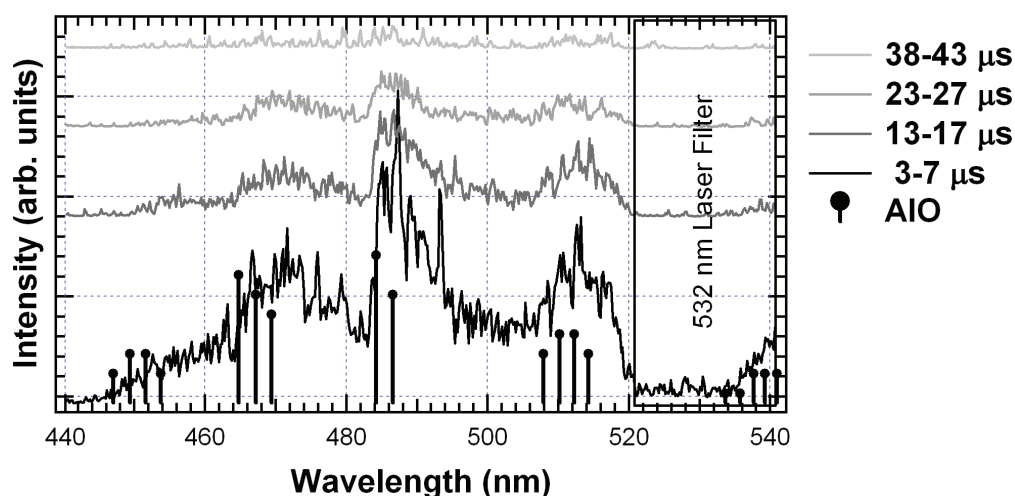


Figure 1 Time resolved emission spectra from the laser initiation of 120.5 nm Al. The line plots were obtained by averaging the spectra within the time ranges shown in the legend. The stick plot was generated from emission lines for AlO obtained from a spectrographic reference.

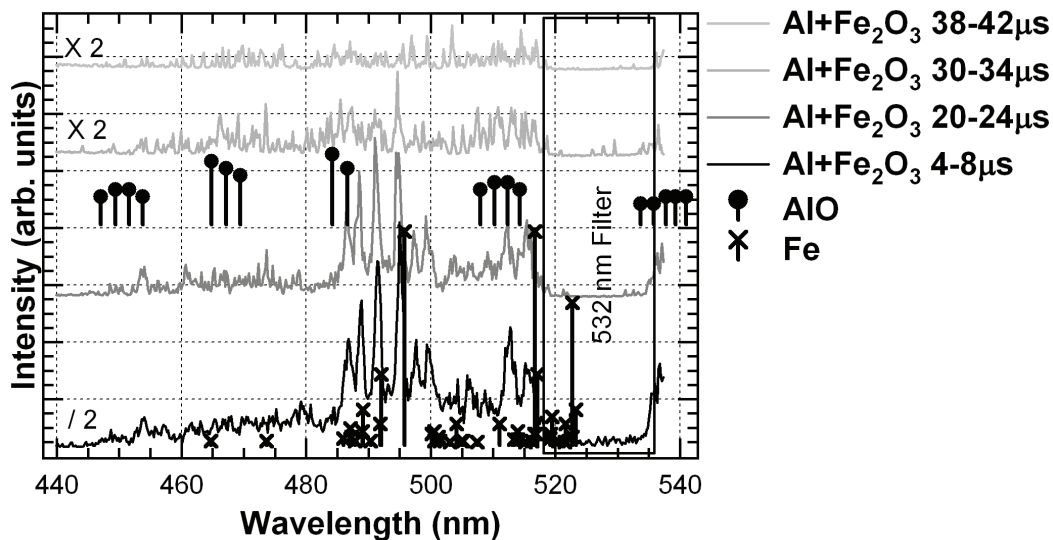


Figure 2 Representative spectra for reaction of Dreizin's $Al + Fe_2O_3$. Each $Al + Fe_2O_3$ line spectrum is an average over the time range shown.

for at least 20 μs . The AlO peaks are visible until 35 μs . Beyond 35 μs there are no spectral features distinguishable above the background noise. Time-averaged spectra from the reaction of Zachariah's $Al + Fe_2O_3$ sample can be seen in Figure 3.

Al + MoO₃

Figure 4 displays a representative set of spectra for the reaction of $Al + MoO_3$ (also prepared by Dreizin's group). During the first 8 μs of the

reaction there is evidence of elemental Mo above the background. This is illustrated by the average of the spectra from 2 to 7 μs shown in Figure 4.

By 9 μs , weak AlO peaks begin to emerge. These peaks gain in intensity, reaching a maximum around 22 μs . The time average of the spectra from 20 to 24 μs is shown in Figure 4. By 40 μs there is still some evidence for AlO peaks, but their intensities are barely above the background noise.

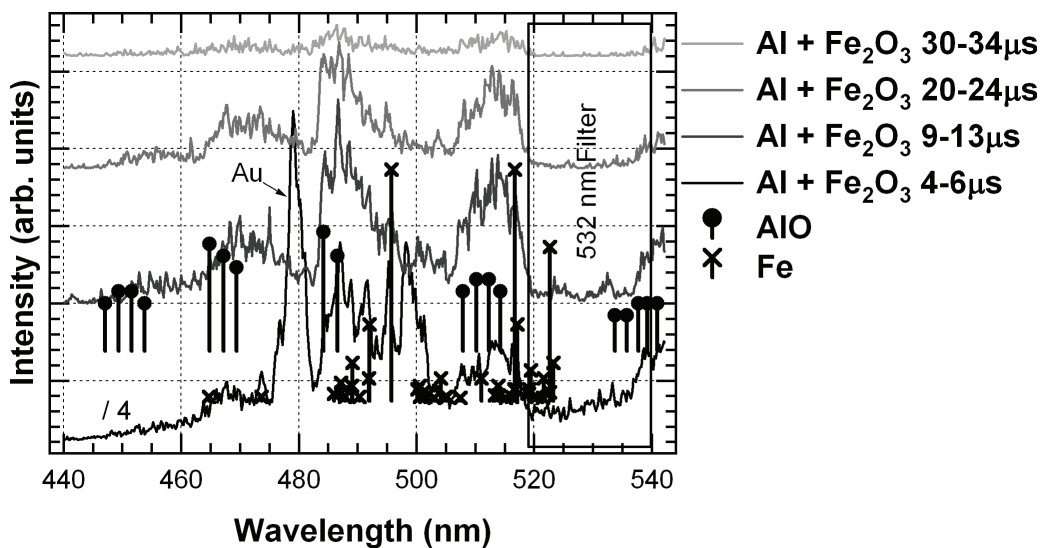


Figure 3 Representative spectra for reaction of Zachariah's $Al + Fe_2O_3$. Each $Al + Fe_2O_3$ line spectrum is an average over the time range shown.

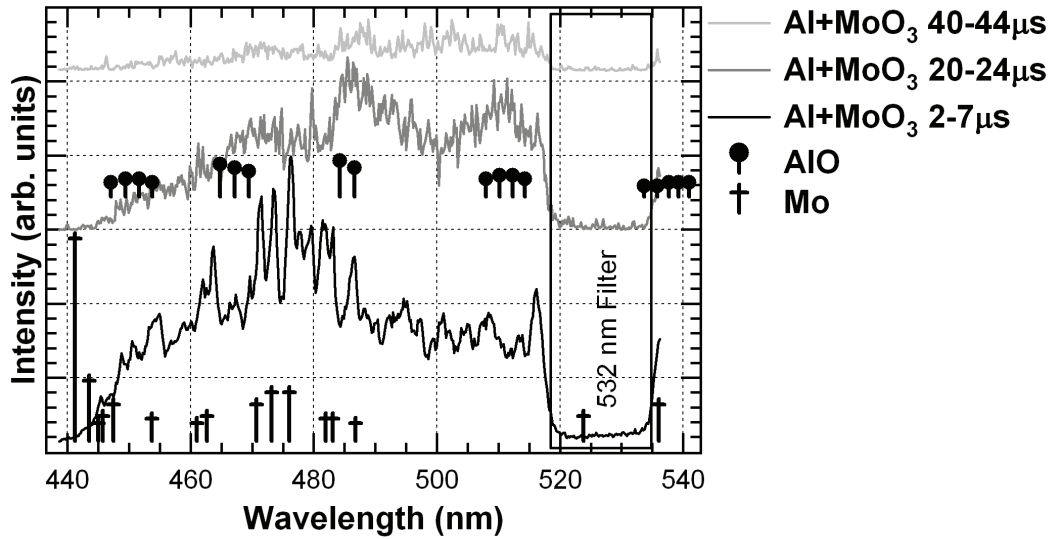


Figure 4 Representative spectra for reaction of Dreizin's $Al + MoO_3$. Each $Al + MoO_3$ line spectrum is an average over the time range shown.

$Al + B_2O_3$

$Al + B_2O_3$ samples were prepared at the South Dakota School of Mines by Jan Puszyński's group.⁹ The laser initiation of $Al + B_2O_3$ produces a more complicated set of spectra with time. For the previous samples, the dominant spectral features visible in this wavelength regime could be attributed to one species or two species that were reasonably well separated in either time or wavelength. In the case of $Al + B_2O_3$ it is

possible that three species are emitting within the same time window. As can be seen in Figure 5, during the first 8 μs there is evidence for AIO emission, but there are other peaks unaccounted for by AIO. In fact, by the 9–13 μs range, the AIO peaks become less intense relative to the rest of the spectrum. The most plausible candidates for the extra spectral features seem to be the oxides of boron. During the 4–8 μs time range evidence for BO is apparent. There is also evidence for

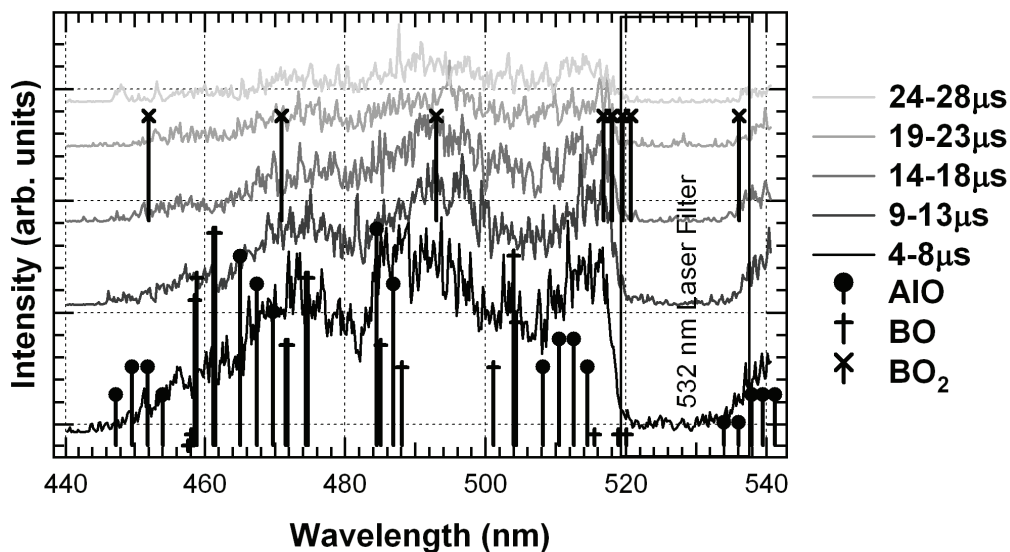


Figure 5 Results of the laser initiation of $Al + B_2O_3$

Table 1 AIO appearance and persistence data from four of the samples studied.

Sample	1 st appearance of AIO (μs)	Final appearance of AIO (μs)
120.5 nm Al	1	41
Al+Fe ₂ O ₃ (Zachariah)	4	37
Al+Fe ₂ O ₃ (Dreizin)	25	38
Al+MoO ₃ (Dreizin)	7	41

peaks of BO₂. The BO₂ peaks appear to increase in intensity and the BO peaks decrease in intensity with time. This suggests that B₂O₃ is not reduced all the way to B, but rather, starts to oxidize again after the initial formation of BO. Apparently the oxidation process for boron is competing with that of aluminum.

Discussion

Table 1 shows a comparison of the AIO appearance and persistence for four of the samples from this study. The Al + B₂O₃ sample is not included because the competing boron oxide signals make it difficult to extract information on the AIO signal by itself. It is important to note that all of these experiments were performed in air. Emission lifetimes would therefore not be limited due to a lack of available oxygen. The significance of the first column relates to the time required for the given material to begin releasing energy from the reaction of aluminum with oxygen. A smaller time in the first column means that the energy will be available earlier. The second column corresponds to the end of energy release due to the formation of AIO. The Al + Fe₂O₃ sample of Zachariah's group showed a slightly delayed AIO emission time as compared to the bare nano Al sample. Most likely there is some time required to break apart the constituents, which contributes to the delay. However, the Dreizin Al + Fe₂O₃ sample shows a significantly different behavior. The time to first appearance of AIO is over 20 μs longer for Dreizin's material. The probable cause for this change comes from the difference in Fe₂O₃ content. It is evident even from visible inspection that the Fe₂O₃ content in Dreizin's sample is much higher than that for Zachariah's. Dreizin's sample has an orange-brown color resulting from excess iron oxide, whereas Zachariah's sample is gray (indicative of the aluminum). The higher Fe₂O₃ content is also illustrated in the persistence of

neutral Fe emission in the spectra. For Zachariah's sample the Fe emission is significantly weakened relative to the AIO emission by 9 μs , while for Dreizin's sample some Fe emission persists beyond 30 μs . Such a strong Fe emission may also mask the original appearance of AIO in the spectra, allowing for the possibility that the AIO emission begins at the same time for both samples but the emission intensity for Dreizin's iron signal overwhelms the weaker AIO signal early in the experiment. For both Al + Fe₂O₃ samples it is clear that the Fe₂O₃ breaks apart early in the reaction. This suggests that this oxide can provide a source of oxygen to the aluminum for reaction.

The Al + MoO₃ sample shows an initial appearance time for AIO similar to that of Zachariah's Al + Fe₂O₃ sample. The initial background is higher for the Al + MoO₃ sample, which may mask any possible earlier detection of AIO. Elemental molybdenum appears above the background, which verifies the release of oxygen.

For the Al + B₂O₃ sample, the AIO signal is convoluted with signals arising from the oxidation of boron. While the original B₂O₃ is most likely breaking apart initially, any released boron appears to be oxidizing at a rate comparable to that of aluminum. The various oxide spectral features begin to appear around 4 μs and last until about 30 μs .

Similar experiments have been performed on RDX with this same experimental method, except a backlight was used to track changes in absorption because the reaction products of RDX do not emit in the visible range available in these experiments. A two-stage process was evident in the RDX reactions. The first stage was the formation of dark intermediate products (evidenced by an increase in absorbance). The second stage was the formation of clear gaseous products (evidenced by

a decrease in absorbance). The time to maximum absorbance for reacting RDX should correspond to the end of the primary reaction zone. The time to maximum absorption for RDX is typically only 3 μ s. The time for the entire reaction of RDX to reach completion is about 13 μ s. Comparing RDX reaction times with those of the samples in Table 1 reveals that only the nano aluminum by itself shows evidence of AlO formation within the time frame of the primary reaction zone of RDX. Zachariah's Al + Fe₂O₃ is close to being within this zone at 4 μ s, followed by Dreizin's Al + MoO₃ (7 μ s). However all of the samples in Table 1, with the exception of Dreizin's Al+Fe₂O₃, would be able to contribute energy from AlO formation to the late time (gaseous) reaction of RDX.

Conclusion

This study reports on the kinetic and chemical processes occurring after the laser initiation in air of 120.5 nm Al, Al + Fe₂O₃, Al + MoO₃, and Al + B₂O₃. All of the samples display spectral features resulting from the combustion of aluminum. AlO emission appears earliest and persists the longest for the nano aluminum sample. The Al + Fe₂O₃ and Al + MoO₃ samples both show emission from the neutral metals of the original oxide (Fe and Mo, respectively) first, followed by the appearance of AlO. This suggests that the metal oxide is breaking down, which provides oxygen for resulting aluminum combustion. However, in these experiments excess oxygen was available from the surrounding air as well. The Al + B₂O₃ showed some evidence for AlO emission, but the AlO spectral features were overlapping and competing with those of BO and BO₂.

Acknowledgements

The authors would like to thank Michael Zachariah, Edward Dreizin and Jan Puszynski for preparing the samples used in this study.

References

- 1 P. Brousseau and C. J. Anderson, "Nanometric Aluminum", *Propellants, Explosives, Pyrotechnics*, vol. 27, 2002, p. 300.
- 2 R. W. Armstrong, B. Baschung, D. W. Booth and M. Samirant, "Enhanced Propellant Combustion with Nanoparticles", *Nano Letters*, vol. 3, 2003, p. 253.
- 3 D. S. Moore, S. F. Son, and B. W. Asay, "Time-Resolved Spectral Emission of Deflagrating Nano-Al and Nano-MoO₃ Metastable Interstitial Composites", *Propellants, Explosives, Pyrotechnics*, vol. 29, 2004, p. 106.
- 4 S. Wang, Y. Yang, Z. Sun, and D. D. Dlott, "Fast Spectroscopy of Energy Release in Nanometric Explosives", *Chemical Physics Letters*, vol. 368, 2003, p. 189.
- 5 NIST Atomic Spectra Database (http://physics.nist.gov/cgi-bin/AtData/main_asd)
- 6 R. W. B. Pearse and A. G. Gaydon, *The Identification of Molecular Spectra*, University Printing House, Cambridge 1976.
- 7 M. Schoenitz, T. Ward and E. L. Dreizin, "Preparation of Energetic Metastable Nano-Composite Materials by Arrested Reactive Milling", *Materials Research Society Proceedings*, vol. 800, 2004, pp. AA2.6.1–AA2.6.6.
- 8 A. Prakash, A. V. McCormick and M. R. Zachariah, "Aero-Sol-Gel Synthesis of Nanoporous Iron-Oxide Particles: A Potential Oxidizer for Nanoenergetic Materials", *Chemistry of Materials*, vol. 16, 2004, p. 1466.
- 9 J. A. Puszynski, "Advances in the Formation of Metal and Ceramic Nanopowders", in *Powder Materials: Current Research and Industrial Practices*, Eds. E. V. Barrera, F. D. S. Marquis and N. N. Thadhani, TMS Current Research and Industrial Practices, TMS, 2001.